ISSN 1070-3284, Russian Journal of Coordination Chemistry, 2022, Vol. 48, No. 12, pp. 902–908. © Pleiades Publishing, Ltd., 2022.

Triphenylantimony(V) Complexes Based on *o*-Aminophenols with the Ambivalent *N*-Aryl Group

A. I. Poddel'sky[a], *, G. K. Fukin[a], and E. V. Baranov[a]

[a] *Razuvaev Institute of Organometallic Chemistry, Russian Academy of Sciences, Nizhny Novgorod, Russia*

**e-mail: aip@iomc.ras.ru*

Received September 6, 2022; revised September 9, 2022; accepted September 9, 2022

Abstract—Triphenylantimony(V) *o*-amidophenolate complexes (AP-OMe)$SbPh_3$ (**I**) and (AP-C(O)Ph)$SbPh_3$ (**II**) have been synthesized from *N*-(2-methoxyphenyl)- and *N*-(2-benzoylphenyl)-4,6-di-*tert*-butyl-*o*-aminophenols. The structures of the complexes in the crystalline state have been determined by X-ray diffraction (XRD) (CIF files CCDC 2205058 (**I**·*n*-hexane) and 2205059 (**II**)). The Sb(1)...O(2) distances in complex **I** (3.018(3) Å) and Sb(1*A*)–O(2*A*) and Sb(1*B*)–O(2*B*) distances in two independent molecules A and B in complex **II** (2.503(3) and 2.878(3) Å, respectively) are less than the sum of the van der Waals radii of the antimony and oxygen atoms, indicating the Sb(1)...O(2) intramolecular interaction. However, the theoretical electron density studies show no interatomic interaction between the antimony atom and the oxygen atom of the methoxy group in the case of complex **I** but confirm these interactions in complex **II.** According to the Espinosa–Molins–Lecomte equation, the energy of these interactions is 11.9 and 4.1 kcal/mol for molecules A and B in complex **II**, respectively.

Keywords: antimony(V), *o*-amidophenolate, XRD, theoretical electron density

DOI: 10.1134/S1070328422700166

INTRODUCTION

Organometallic and coordination antimony derivatives are attractive objects for investigation, since they demonstrate diverse and sometimes unusual structures and reactivity [1–9] and also have a high potential of applying as components of catalysts for various reactions of organic chemistry, as reagents in fine organic and organoelement synthesis [10–13], and in medicine [14–17]. The antimony(V) complexes with the redox-active ligands of the *o*-quinone/*o*-iminoquinone type are interesting from the viewpoint of their reactivity: they are used as traps of halide anions, sensors to halide anions [18, 19], nontrivial ligands in the coordination chemistry of transition metals [20], reversible fixators for molecular oxygen [21–25], interceptors of radicals (including those in biochemical processes) [26–30], and others.

Coordination chemistry of *o*-iminoquinone ligands with additional functional groups has intensively been developed in the recent years [31–36]. This is related to the fact that similar ligands allow one not only to change the structure of the internal coordination sphere of the metal but make the change purposeful and controllable, including that depending on the external conditions (e.g., by changing the reduction state of the ligand and oxidation state of the metal). As a result, directed changes in the magnetic properties of the complexes and in their chemical behavior also occur. In this work, we synthesized triphenylantimony(V) *o*-aminophenolate complexes with additional functional groups (methoxy and benzoyl) in the *N*-aryl substituent and studied their structures.

EXPERIMENTAL

The solvents used were purified according to standard procedures [37, 38]. *o*-Aminophenols L^1 and L^2 were synthesized using known procedures [36, 39]. ^1H and ^{13}C NMR spectra were recorded on a Bruker DPX 200 spectrometer (frequency 200 MHz (^1H), 50 MHz (^{13}C); internal standard tetramethylsilane, solvent $CDCl_3$). Elemental analysis (C, H, Sb) was carried out by the pyrolytic method.

The complexes were synthesized in evacuated ampules in the absence of oxygen and moisture using the following procedures: a solution of the corresponding *o*-aminophenol (0.5 mmol, 20 mL of toluene) was added to a solution of triphenylantimony dibromide (0.260 g, 0.5 mmol, 25 mL of toluene) at room temperature with stirring. After *o*-aminophenol was added completely, a solution (0.15 mL) of triethylamine (1 mmol) in toluene (10 mL) was poured to the resulting solution with stirring. The solution turned turbid, and a precipitate of the ammonium salt formed. The reaction mixture was stirred additionally for 1 h at room temperature, and the precipitate was

filtered off on a vacuum filter. Toluene was removed in vacuo from the obtained yellow solution, the solid residue was dissolved in warm (~50°C) *n*-hexane (30 mL), and the formed yellow-orange solution was left at −18°C for 24 h. The formed fine crystalline precipitates were filtered off and dried in vacuo. Complexes **I** and **II** were obtained as crystalline light yellow powders sensitive to oxygen. The yield of complex **I** was 0.27 g (79%). The yield of complex **II** was 0.29 g (77%). The crystals of the complexes suitable for XRD were grown from mother liquors in *n*-hexane at −18°C for 5 days.

For (4,6-di-*tert*-butyl-*N*-(2-methoxyphenyl)-*o*-amidophenolato)triphenylantimony(V) (**I**):

^{1}H NMR (200 MHz; δ, ppm): 1.18 (s, 9H, ^{t}Bu), 1.49 (s, 9H, ^{t}Bu), 3.30 (s, 3H, OMe), 6.24 (d, $^4J_{(H,H)}$ = 2.0 Hz, 1H, arom. C_6H_2), 6.34 (s, $^3J_{(H,H)}$ = 8.0 Hz, 1H, arom. C_6H_4), 6.70 (dt, $^3J_{(H,H)}$ = 7.5 Hz, $^4J_{(H,H)}$ = 1.2 Hz, 1H, atom. C_6H_4), 6.85 (dm, $^3J_{(H,H)}$ = 7.8 Hz, 1H, arom. C_6H_4), 6.78 (d, $^4J_{(H,H)}$ = 2.0 Hz, 1H, arom. C_6H_2), 7.07 (dt, $^3J_{(H,H)}$ = 7.8 Hz, $^4J_{(H,H)}$ = 1.2 Hz, 1H, arom. C_6H_4), 7.20–7.40 (m, 9H, Ph), 7.50–7.62 (m, 6H, Ph).

^{13}C NMR (50 MHz; δ, ppm): 29.96, 31.82, 34.32, 34.78, 54.42, 107.27, 110.47, 112.36, 120.17, 126.81, 128.06, 129.45, 129.90, 131.60, 133.82, 135.33, 136.69, 137.27, 139.27, 146.32, 155.63.

For $C_{39}H_{42}NO_2Sb$

Anal. calcd., %	C, 69.04	H, 6.24	Sb, 17.95
Found, %	C, 68.89	H, 6.18	Sb, 18.12

For (4,6-di-*tert*-butyl-*N*-(2-benzoylphenyl)-*o*-amidophenolato)triphenylantimony(V) (**II**):

^{1}H NMR (200 MHz; δ, ppm): 1.07 (s, 9H, ^{t}Bu), 1.38 (s, 9H, ^{t}Bu), 6.08 (d, $^4J_{(H,H)}$ = 2.3 Hz, 1H, arom. C_6H_2), 6.54 (d, $^4J_{(H,H)}$ = 2.3 Hz, 1H, arom. C_6H_2), 6.85–7.05 (m, 2H, arom. C_6H_4), 7.07–7.17 (m, 2H, Ph), 7.20–7.38 (m, 11H, Ph and arom. C_6H_4), 7.40–7.48 (m, 1H, Ph), 7.50–7.60 (m, 2H, Ph), 7.62–7.78 (m, 6H, Ph).

^{13}C NMR (50 MHz; δ, ppm): 29.75, 31.75, 34.13, 34.60, 109.90, 112.77, 124.28, 127.82, 127.98, 129.35, 130.50, 130.63, 131.18, 131.95, 132.80, 134.87, 135.01, 135.33, 136.64, 137.25, 138.81, 141.53, 145.44, 149.04, 197.02.

For $C_{45}H_{44}NO_2Sb$

Anal. calcd., %	C, 71.82	H, 5.89	Sb, 16.18
Found, %	C, 71.90	H, 5.97	Sb, 16.05

XRD. Diffraction data for crystals of compounds **I** and **II** were collected on an Oxford Xcalibur Eos single-crystal X-ray diffractometer at 100 K. Experimental sets of intensities were integrated using the CrysAlisPro program [40]. The structures were solved by a direct method and refined by full-matrix least squares for F^2_{hkl} in the anisotropic approximation for all non-hydrogen atoms in the SHELXTL program package [41]. Hydrogen atoms were placed in the geometrically calculated positions and refined isotropically. An absorption correction was applied using the SCALE3 ABSPACK program [40]. One of the *tert*-butyl groups in compound **I**, one *tert*-butyl group in the first independent molecule of compound **II**, and the phenyl ring of the benzoyl group in the second independent molecule of compound **II** were disordered over two positions. The solvate molecule of *n*-hexane disordered over three positions was found in the crystal of compound **I** in the 1 : 2 ratio to the antimony complex. The crystallographic data and X-ray experimental and structure refinement parameters for the complexes are given in Table 1. The structural data were deposited with the Cambridge Crystallographic Data Centre (CIF files CCDC 2205058 (**I**·*n*-hexane) and 2205059 (**II**); deposit@ccdc.cam.ac.uk; http://www.ccdc.cam.ac.uk).

Theoretical electron density. One-point DFT calculations of the periodical three-dimensional structures of complexes **I** and **II** were performed in the framework of the B3LYP exchange correlation potential [42, 43] in the CRYSTAL17 program [44] using the DGDZVP full-electron basis set [45–48]. The atomic coordinates for the one-point DFT calculation were taken from the data of routine XRD experiments for compounds **I** and **II**. The contraction coefficient of reciprocal space was established to be four, which corresponded to 30 K points in the irreducible Brillouin zone in which the Hamiltonian matrix was diagonalized.

The PLATON program (version 60119) [49] was applied to generate 98274 and 52949 independent Miller indices *hkl* for compounds **I** and **II** with the reverse resolution to $s = 1.16$ Å^{-1}. The XFAC option of the CRYSTAL17 program was used to obtain a set of theoretical structural factors F_{hkl} from the electron density function determined by the one-point calculations of the non-optimized crystal structures of compounds **I** and **II**.

The populations of the spherically symmetric valence shell (P_{val}) and multipole parameters (P_{lm}) describing its deformation along with the corresponding expansion–contraction coefficients (k, k') were obtained for each atom of complexes **I** and **II** from the calculated structural amplitudes F_{hkl} using the MoPro program [50] in terms of the Hansen–Coppens multipole formalism [51]. Prior to multipole refinement, the C–H bond lengths were normalized to the values obtained from the neutron diffraction data [52]. The multipole expansion levels were hexadecapole for the

antimony atom and octapole for all other atoms except for hydrogen atoms, and one dipole level was used for hydrogen atoms. The obtained values of P_{val}, P_{lm}, k, and k' were used for the construction of the theoretical electron density. The topology of the theoretical function ρ(r) was analyzed using the WINXPRO software [53].

RESULTS AND DISCUSSION

The triphenylantimony(V) *o*-amidophenolate complexes (AP-OMe)$SbPh_3$ (**I**) and (AP-C(O)Ph)$SbPh_3$ (**II**) were synthesized by the exchange reactions of triphenylantimony dibromide with the corresponding *o*-aminophenol (L^1 and L^2) and two equivalents of triethylamine (Scheme 1).

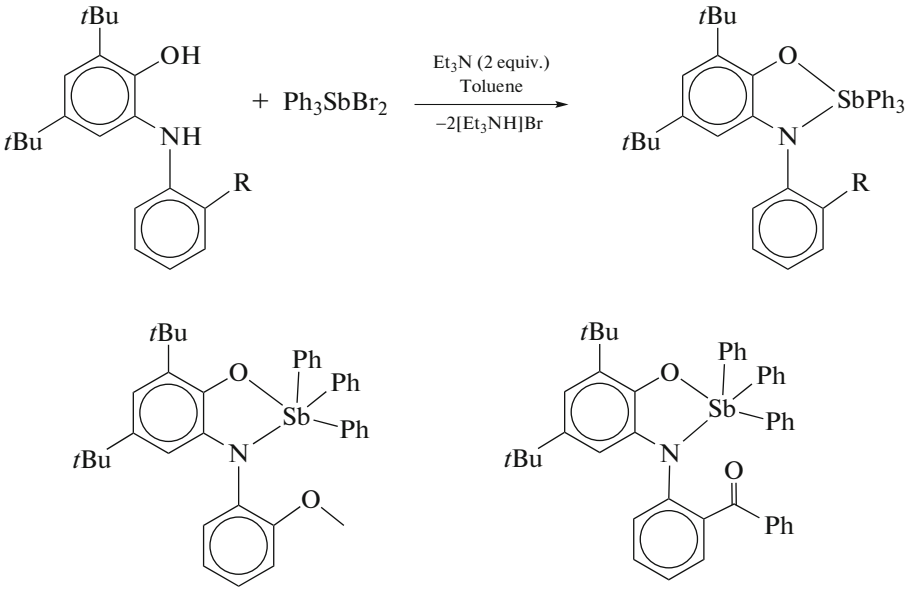

Scheme 1.

In the solid state, compounds **I** and **II** are finely crystalline light yellow powders sensitive to oxygen. The complexes were characterized from the data of ^1H and ^{13}C NMR spectroscopy and elemental analysis. The molecular structures of the complexes in the crystalline state were determined by XRD.

According to the XRD data (Fig. 1), in methoxy-containing *o*-amidophenolate (AP-OMe)$SbPh_3$ **I**, antimony exists in a distorted trigonal bipyramidal environment. The base of the pyramid is formed of the N(1), C(28), and C(34) atoms. The sum of the bond angles N(1)–Sb(1)–C(34), C(34)–Sb(1)–C(28), and N(1)–Sb(1)–C(28) is 357.04°. The Sb(1)–C(22) bond with the apical phenyl group is longer than the equatorial Sb(1)–C(28) and Sb(1)–C(34) bonds by 0.03–0.04 Å. The O(1)–Sb(1)–C(22) angle is 171.46(8)°. The parameter applied for the quantitative description of the coordination polyhedron of the complexes with the coordination number 5 is $\tau = 0.72$ (in an ideal trigonal bipyramid, $\tau = 1$; in an ideal tetragonal pyramid, $\tau = 0$ [54]). Similar distinctions in lengths of the bond around the central antimony atom and close values of τ were found earlier for the related triarylphenylantimony(V) catecholates of the distorted trigonal bipyramidal structure [55–57]. The O(1)–C(1) and N(1)–C(2) bonds (1.354(3) and 1.408(3) Å, respectively) correspond to these ordinary bonds in a series of other *o*-amidophenolate complexes of antimony(V) [21, 23, 58, 59] and other metals [60–62], and the six-membered carbon ring C(1–6) is aromatic with an average C–C bond length of 1.400 ± 0.008 Å.

A weak intramolecular interaction is observed between the O(2) oxygen of the methoxy group and central antimony atom Sb(1) in the molecule of complex **I** in the crystalline form. The Sb(1)...O(2) distance is 3.018(3) Å, which considerably exceeds the observed similar distances in antimony(V) catecholates with coordinated alkoxy groups (e.g., 2.4207(11) Å in (6-$HexOCH_2$-3,5-DBCat)$SbPh_3$·2MeOH [63]) but is less than the sum of the van der Waals radii of antimony and oxygen (2.2 and 1.5 Å [64]; 2.06 and 1.52 Å [65]). Similar short contacts Sb···OMe (2.808(2)–3.152(2) and 2.933(3)–3.082(3) Å in tris(2-methoxyphenyl)antimony(V) 3-carboxycatecholate and 4-carboxycatecholate, respectively) were also observed [66]. The crystalline cell of *o*-amidophenolate **II** contains two independent molecules A and B of the complex (Figs. 2 and 3, respectively) with somewhat different structures.

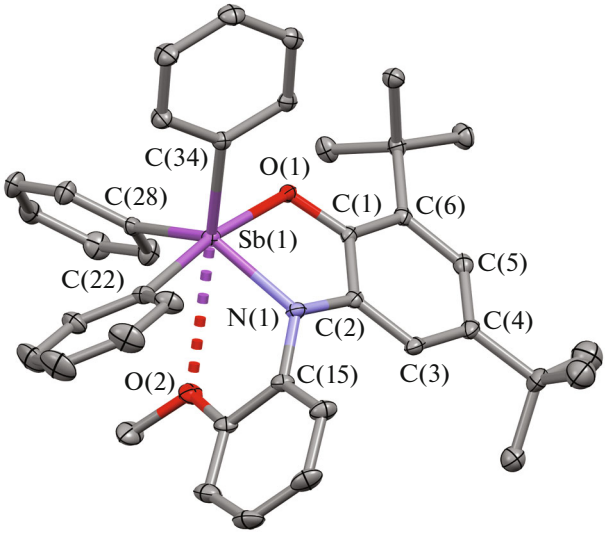

Fig. 1. Molecular structure of *o*-amidophenolate (AP-OMe)$SbPh_3$ (**I**) according to the XRD data (hydrogen atoms are omitted). Selected bond lengths (Å) and bond angles (°): Sb(1)–O(1) 2.0764(15), Sb(1)–N(1) 2.0489(19), Sb(1)–C(22) 2.160(2), Sb(1)–C(28) 2.127(2), Sb(1)–C(34) 2.121(2), Sb(1)...O(3) 3.018(3), O(1)–C(1) 1.354(3), N(1)–C(2) 1.408(3), N(1)–C(15) 1.421(3), C(1)–C(2) 1.408(3), C(1)–C(6) 1.403(3), C(2)–C(3) 1.392(3), C(3)–C(4) 1.397(4), C(4)–C(5) 1.394(4), and C(5)–C(6) 1.405(3); N(1)–Sb(1)–O(1) 78.11(7), N(1)–Sb(1)–C(34) 115.37(8), C(34)–Sb(1)–C(28) 113.28(8), N(1)–Sb(1)–C(28) 128.39(8), and O(1)–Sb(1)–C(22) 171.46(8).

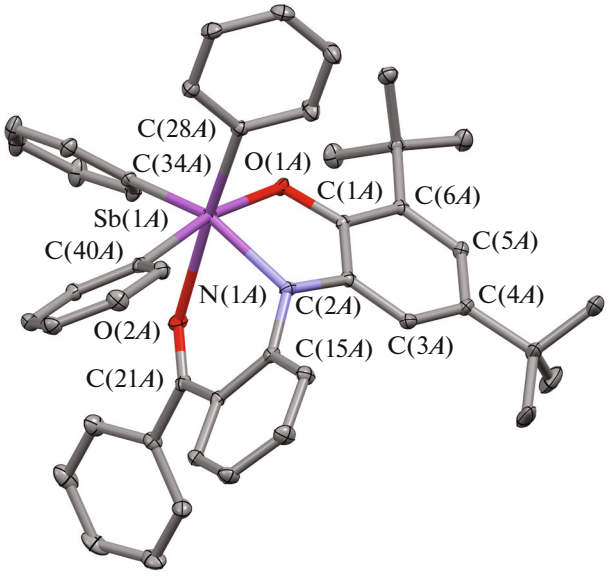

Fig. 2. Structure of molecule A in the crystal of (AP-C(O)Ph)$SbPh_3$ (**II**) according to the XRD data (hydrogen atoms are omitted). Selected bond lengths (Å) and bond angles (°): Sb(1*A*)–O(1*A*) 2.0612(14), Sb(1*A*)–N(1*A*) 2.0711(18), Sb(1*A*)–C(28*A*) 2.137(2), Sb(1*A*)–C(34*A*) 2.130(2), Sb(1*A*)–C(40*A*) 2.160(2), Sb(1*A*)–O(2*A*) 2.5025(15), O(1*A*)–C(1*A*) 1.358(2), O(2*A*)–C(21*A*) 1.234(3), N(1*A*)–C(2*A*) 1.407(3), N(1*A*)–C(15*A*) 1.405(3), C(1*A*)–C(2*A*) 1.411(3), C(1*A*)–C(6*A*) 1.408(3), C(2*A*)–C(3*A*) 1.392(3), C(3*A*)–C(4*A*) 1.390(3), C(4*A*)–C(5*A*) 1.400(3), and C(5*A*)–C(6*A*) 1.404(3); O(1*A*)–Sb(1*A*)–N(1*A*) 78.37(6), N(1*A*)–Sb(1*A*)–C(34*A*) 146.20(8), O(1*A*)–Sb(1*A*)–C(40*A*) 169.52(7), C(28*A*)–Sb(1*A*)–O(2*A*) 176.52(7), O(1*A*)–Sb(1*A*)–O(2*A*) 89.71(5), N(1*A*)–Sb(1*A*)–O(2*A*) 73.06(6), C(34*A*)–Sb(1*A*)–O(2*A*) 76.18(7), and C(40*A*)–Sb(1*A*)–O(2*A*) 82.74(6).

The geometric characteristics of the O,N-chelating moieties O(1*A*)N(1*A*)C(1*A*–6*A*) and O(1*B*)N(1*B*)-C(1*B*–6*B*) of the ligands correspond to those for the earlier studied *o*-amidophenolate complexes [21, 23, 58, 59, 67]. The distances Sb(1)–C(28), Sb(1)–C(34), and Sb(1)–C(40) (2.130–2.160(2) Å in molecule A; 2.134(2)–2.146(2) Å in molecule B) and Sb(1)–O(1) and Sb(1)–N(1) (2.0612(14), 2.0711(18) Å in molecule A; 2.0716(15), 2.0534(18) Å in molecule B, respectively) are also typical of the antimony *o*-amidophenolate complexes [21, 23, 58, 59]. The coordination sphere of the central antimony atom in both independent molecules A and B is supplemented to 6 due to the interaction between the central antimony atom Sb(1) and the oxygen atom O(2) of the carbonyl group of the benzoyl substituent in *N*-aryl. The Sb(1*A*)...O(2*A*) and Sb(1*B*)...O(2*B*) distances differ significantly: the Sb(1*A*)–O(2*A*) distance is 2.503(3) Å, whereas the Sb(1*B*)–O(2*B*) distance is 2.878(3) Å. In molecule A, this bond is close to a similar bond between the central antimony atom and the oxygen atom of the acetone molecule in the (3,6-DBCat)Sb(*p*-Cl-Ph)$_3$ complex (2.497(15) Å) [68].

As mentioned above, the sum of the van der Waals radii of the antimony and oxygen atoms shows the intramolecular Sb(1)...O(2) interaction (3.018(3) Å) in complex **I**. We decided to check this conclusion from the viewpoint of theoretical electron density. As can be seen from Fig. 4, the theoretical molecular graph of complex **I** contains no bond path and critical point (3, –1) (CP(3, –1)) between the Sb(1) and O(2) atoms.

According to Bader's theory [69], the absence of the bond path and CP(3, –1) indicates the absence of interatomic interactions. However, Bader's theory does not always reproduce all expected bond paths and CP(3, –1). This situation is observed most frequently in the complexes containing π-carbocyclic ligands [70–73], because the electron density curvatures between the metal atom and ligand is very low in these complexes. We have recently proposed to use an approach for a system with a low electron density curvature [74, 75] based on the simultaneous use of the source function [76–78] and index of noncovalent interactions [79–81]. In this approach, we propose to use the isosurface of the index of noncovalent interactions to choose points for comparison of the source function. The use of the approach showed no interaction between the Sb(1) and O(2) atoms in complex **I**.

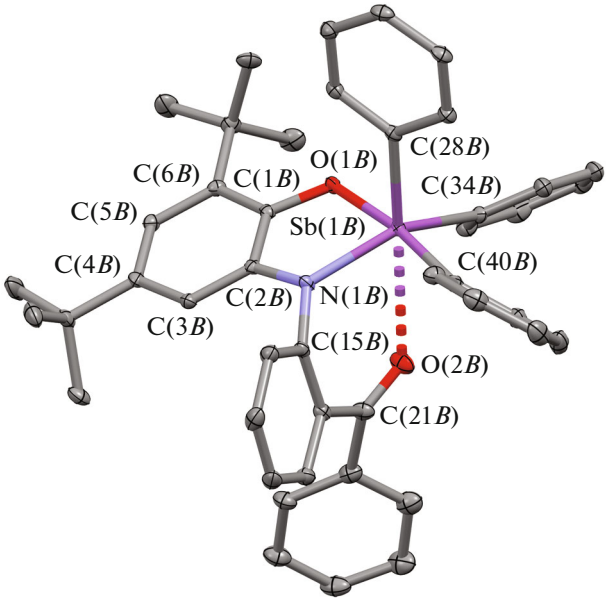

Fig. 3. Structure of molecule B in the crystal of (AP-C(O)Ph)$SbPh_3$ (**II**) according to the XRD data (hydrogen atoms are omitted). Selected bond lengths (Å) and bond angles (°): Sb(1*B*)–O(1*B*) 2.0716(15), Sb(1*B*)–N(1*B*) 2.0534(18), Sb(1*B*)–C(28*B*) 2.134(2), Sb(1*B*)–C(34*B*) 2.135(2), Sb(1*B*)–C(40*B*) 2.146(2), Sb(1*B*)–O(2*B*) 2.8778(18), O(1*B*)–C(1*B*) 1.355(3), O(2*B*)–C(21*B*) 1.219(3), N(1*B*)–C(2*B*) 1.413(3), N(1*B*)–C(15*B*) 1.425(3), C(1*B*)–C(2*B*) 1.404(3), C(1*B*)–C(6*B*) 1.400(3), C(2*B*)–C(3*B*) 1.389(3), C(3*B*)–C(4*B*) 1.403(3), C(4*B*)–C(5*B*) 1.391(3), and C(5*B*)–C(6*B*) 1.412(3); O(1*B*)–Sb(1*B*)–N(1*B*) 78.16(6), N(1*B*)–Sb(1*B*)–C(34*B*) 141.06(8), O(1*B*)–Sb(1*B*)–C(40*B*) 172.45(7), C(28*B*)–Sb(1*B*)–O(2*B*) 175.49(7), O(1*B*)–Sb(1*B*)–O(2*B*) 93.73(6), N(1*B*)–Sb(1*B*)–O(2*B*) 68.59(6), C(340*B*)–Sb(1*B*)–O(2*B*) 77.70(7), and C(40*B*)–Sb(1*B*)–O(2*B*) 82.29(7).

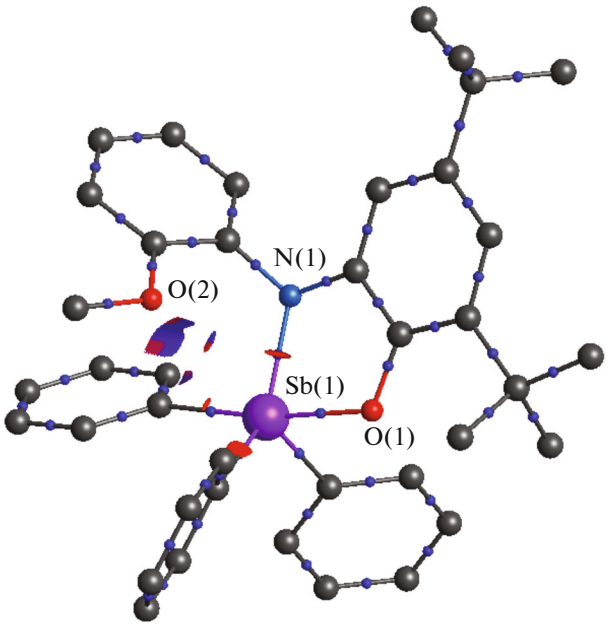

Fig. 4. Theoretical molecular graph and isosurface (0.17 a.u.) of the index of noncovalent interactions in complex **I**. Only CP(3, –1) are shown.

In turn, the intramolecular Sb(1*A*,*B*)...O(2*A*,*B*) interactions are observed in complex **II** (Fig. 5). According to the Espinosa–Molins–Lecomte equation [82], the energy of these interactions is 11.9 (2.503(3) Å) and 4.1 (2.878(3) Å) kcal/mol for molecules A and B of complex **II**, respectively. Thus, a distance of ~3 Å can be considered to be a conventional boundary of the presence/absence of interactions between the Sb(V) and oxygen atoms.

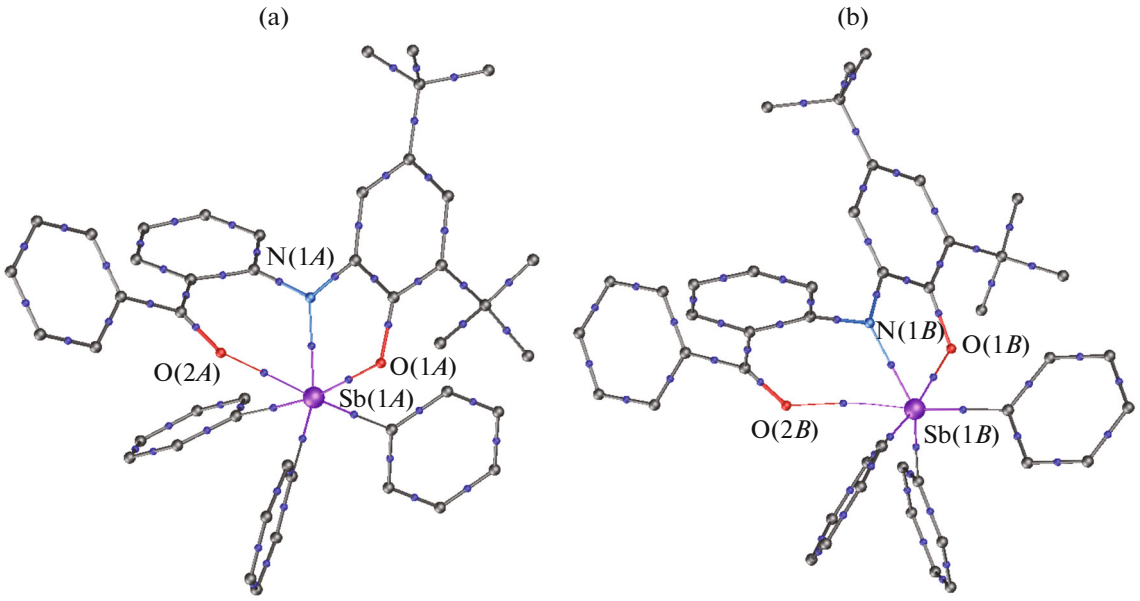

Fig. 5. Theoretical molecular graph for complex **II**. Only CP(3, –1) are shown.

FUNDING

This work was supported by the Russian Science Foundation, project no. 21-13-00336.

CONFLICT OF INTEREST

The authors declare that they have no conflicts of interest.

REFERENCES

1. Sharutin, V.V., Poddel'sky, A.I., and Sharutina, O.K., *Russ. J. Coord. Chem.*, 2020, vol. 46, p. 663.
2. Christianson, A.M. and Gabbai, F.P., *Chem. Commun.*, 2017, vol. 53, p. 2471.
3. Lin, T.-P., Wade, C.R., Perez, L.M., and Gabbai, F.P., *Angew. Chem., Int. Ed. Engl.*, 2010, vol. 49, p. 6357.
4. Wade, C.R. and Gabbaï, F.P., *Angew. Chem., Int. Ed. Engl.*, 2011, vol. 50, p. 7369.
5. Sahu, S. and Gabbai, F.P., *J. Am. Chem. Soc.*, 2017, vol. 139, p. 5035.
6. Tofan, D. and Gabbaï, F.P., *Chem. Sci.*, 2016, vol. 7, p. 6768.
7. Raţ, C.I., Silvestru, C., and Breunig, H.J., *Coord. Chem. Rev.*, 2013, vol. 257, p. 818.
8. Smith, J.E., Yang, H., and Gabbaï, F.P., *Organometallics*, 2021, vol. 40, p. 3886.
9. Balázs, L. and Breunig, H.J., *Coord. Chem. Rev.*, 2004, vol. 248, p. 603.
10. Chen, Y., Qiu, R., Xu, X., et al., *RSC Adv.*, 2014, vol. 4, p. 11907.
11. You, D. and Gabbaï, F.P., *J. Am. Chem. Soc.*, 2017, vol. 139, p. 6843.
12. You, D., Yang, H., Sen, S., and Gabbaï, F.P., *J. Am. Chem. Soc.*, 2018, vol. 140, p. 9644.
13. Hirai, M., Cho, J., and Gabbaï, F.P., *Chem. - Eur. J.*, 2016, vol. 22, p. 6537.
14. Ali, M.I., Rauf, M.K., Badshah, A., et al., *Dalton Trans.*, 2013, vol. 42, p. 16733.
15. Sharma, P., Perez, D., Cabrera, A., et al., *Acta Pharmacol. Sin.*, 2008, vol. 29, p. 881.
16. Adeyemi, J.O. and Onwudiwe, D.C., *Molecules*, 2020, vol. 25, no. 2, p. 305.
17. Frézard, F., Demicheli, C., Kato, K.C., et al., *Rev. Inorg. Chem.*, 2013, vol. 33, p. 1.
18. Christianson, A.M. and Gabbai F.P., *Antimony- and Bismuth-Based Materials and Applications*, In: *Main Group Strategies Towards Functional Organic Materials*, Baumgartner, T. and Jaekle, F., Eds., Wiley, 2017, vol. 16, p. 405.
19. Hirai, M. and Gabbaï, F.P., *Angew. Chem., Int. Ed. Engl.*, 2015, vol. 127, p. 1221.
20. Jones, J.S. and Gabbaï, F.P., *Acc. Chem. Res.*, 2016, vol. 49, p. 857.
21. Abakumov, G.A., Poddel'sky, A.I., Grunova, E.V., et al., *Angew. Chem., Int. Ed. Engl.*, 2005, vol. 44, p. 2767.
22. Abakumov, G.A., Cherkasov, V.K., Grunova E.V., et al., *Dokl. Akad. Nauk*, 2005, vol. 405, p. 199.
23. Cherkasov, V.K., Abakumov, G.A., Grunova, E.V., et al., *Chem. - Eur. J.*, 2006, vol. 12, p. 3916.
24. Fukin, G.K., Baranov, E.V., Jelsch, C., et al., *J. Phys. Chem. A*, 2011, vol. 115, p. 8271.
25. Poddel'sky, A.I., Smolyaninov, I.V., Kurskii, Yu.A., et al., *J. Organomet. Chem.*, 2010, vol. 695, p. 1215.
26. Smolyaninov, I.V., Antonova, N.A., Poddel'sky, A.I., et al., *J. Organomet. Chem.*, 2011, vol. 696, p. 2611.
27. Smolyaninov, I.V., Antonova, N.A., Poddel'skii, A.I., et al., *Dokl. Akad. Nauk*, 2012, vol. 443, p. 64.
28. Smolyaninov, I.V., Antonova, N.A., Poddel'sky, A.I., et al., *Appl. Organomet. Chem.*, 2012, vol. 26, p. 277.
29. Smolyaninov, I.V., Poddel'skii, A.I., Antonova, N.A., et al., *Russ. J. Coord. Chem.*, 2013, vol. 39, p. 165. https://doi.org/10.1134/S1070328413020073
30. Smolyaninov, I.V., Antonova, N.A., Poddel'sky, A.I., et al., *Appl. Organomet. Chem.*, 2014, vol. 28, p. 274.
31. Ye, S., Sarkar, B., Lissner, F., et al., *Angew. Chem., Int. Ed. Engl.*, 2005, vol. 44, p. 2103.
32. Kaim, W. and Paretzki, A., *Coord. Chem. Rev.*, 2017, vol. 344, p. 345.
33. Hübner, R., Weber, S., Strobel, S., et al., *Organometallics*, 2011, vol. 30, p. 1414.
34. Piskunov, A.V., Pashanova, K.I., Bogomyakov, A.S., et al., *Dalton Trans.*, 2018, vol. 47, p. 15049.
35. Piskunov, A.V., Pashanova, K.I., Ershova, I.V., et al., *J. Mol. Struct.*, 2018, vol. 1165, p. 51.
36. Piskunov, A.V., Pashanova, K.I., Bogomyakov, A.S., et al., *Polyhedron*, 2016, vol. 119, p. 286.
37. Gordon, A. and Ford, R., *The Chemist's Companion: A Handbook of Practical Data, Techniques, and References*, New York: Wiley, 1972.
38. Perrin, D.D., Armarego, W.L.F., and Perrin, D.R., *Purification of Laboratory Chemicals*, Oxford: Pergamon, 1980.
39. Ghorai, S. and Mukherjee, C., *Chem. Commun.*, 2012, vol. 48, p. 10180.
40. *Rigaku Oxford Diffraction. 2015. CrysAlis Pro Software System, version 1.171.38.46*, Wroclaw: Rigaku.
41. Sheldrick, G.M., *Acta Crystallogr., Sect. C: Struct. Chem.*, 2015, vol. 71, p. 3.
42. Becke, A.D., *J. Chem. Phys.*, 1993, vol. 98, p. 5648.
43. Lee, C., Yang, W., and Parr, R.G., *Phys. Rev.*, 1988, vol. 37, p. 785.
44. Dovesi, R., Erba, A., Orlando, R., et al., *WIREs Comput. Mol. Sci.*, 2018, vol. 8, p. e1360.
45. Godbout, N., Salahub, D.R., Andzelm, J., et al., *Can. J. Chem.*, 1992, vol. 70, p. 560.
46. Pritchard, B.P., Altarawy, D., Didier, B., et al., *J. Chem. Inf. Model*, 2019, vol. 59, p. 4814.
47. Feller, D., *J. Comput. Chem.*, 1996, vol. 17, p. 1571.
48. Schuchardt, K.L., Didier, B.T., Elsethagen, T., et al., *J. Chem. Inf. Model*, 2007, vol. 47, p. 1045.
49. Spek, A.L., *Acta Crystallogr., Sect. C: Cryst. Chem.*, 2015, vol. 71, p. 9.
50. Jelsch, C., Guillot, B., Lagoutte, A., et al., *J. Appl. Crystallogr.*, 2005, vol. 38, p. 38.

51. Hansen, N.K. and Coppens, P., *Acta Crystallogr., Sect. A: Cryst. Phys., Diffr., Theor. Gen. Crystallogr.*, 1978, vol. 34, p. 909.
52. Allen, F.H., Kennard, O., Watson, D.G., et al., *J. Chem. Soc., Perkin Trans.*, 1987, vol. 2, p. 1.
53. Stash, A.I. and Tsirelson, V.G., *J. Appl. Crystallogr.*, 2014, vol. 47, p. 2086.
54. Addison, A.W., Rao, T.N., Reedijk, J., et al., *J. Chem. Soc., Dalton Trans.*, 1984, p. 1349.
55. Poddel'sky, A.I., Baranov, E.V., Fukin, G.K., et al., *J. Organomet. Chem.*, 2013, vol. 733, p. 44.
56. Poddel'sky, A.I., Smolyaninov, I.V., Druzhkov, N.O., et al., *J. Organomet. Chem.*, 2021, vol. 952, p. 121994.
57. Poddel'sky, A.I., Smolyaninov, I.V., Berberova, N.T., et al., *J. Organomet. Chem.*, 2015, vols. 789–790, p. 8.
58. Poddel'sky, A.I., Vavilina, N.N., Somov, N.V., et al., *J. Organomet. Chem.*, 2009, vol. 694, p. 3462.
59. Poddel'sky, A.I., Kurskii, Yu.A., Piskunov, A.V., et al., *Appl. Organomet. Chem.*, 2011, vol. 25, p. 180.
60. Klementyeva, S.V., Lukoyanov, A.N., Afonin, M.Yu., et al., *Dalton Trans.*, 2019, vol. 48, p. 3338.
61. Piskunov, A.V., Aivaz'yan, I.A., Fukin, G.K., et al., *Inorg. Chem. Commun.*, 2006, vol. 9, p. 612.
62. Piskunov, A.V., Aivaz'yan, I.A., Poddel'sky, A.I., et al., *Eur. J. Inorg. Chem.*, 2008, p. 1435.
63. Poddel'sky, A.I., Astaf'eva, T.V., Smolyaninov, I.V., et al., *J. Organomet. Chem.*, 2018, vol. 873, p. 57.
64. Batsanov, S.S., *Zh. Neorg. Khim.*, 1991, vol. 36, p. 3015.
65. Mantina, M., Chamberlin, A.C., Valero, R., et al., *J. Phys. Chem. A*, 2009, vol. 113, p. 5806.
66. Sharutin, V.V., Sharutina O.K., and Belov, V.V., *Russ. J. Coord. Chem.*, 2022, in press.
67. Fukin, G.K., Baranov, E.V., Poddel'sky, A.I., et al., *ChemPhysChem*, 2012, vol. 13, p. 3773.
68. Poddel'sky, A.I., Smolyaninov, I.V., Fukin, G.K., et al., *J. Organomet. Chem.*, 2018, vol. 867, p. 238.
69. Bader, R.F.W., *Atoms in Molecules. A Quantum Theory*, Oxford: Clarendron, 1990.
70. Farrugia, L.J., Evans, C., Lentz, D., et al., *J. Am. Chem. Soc.*, 2009, vol. 131, p. 1251.
71. Fukin, G.K., Cherkasov, A.V., Baranov, E.V., et al., *ChemistrySelect*, 2019, vol. 4, p. 1.
72. Smol'yakov, A.F., Dolgushin, F.M., and Antipin, M.Yu., *Russ. Chem. Bull.*, 2012, vol. 61, p. 2204.
73. Smol'yakov, A.F., Dolgushin, F.M., Ginzburg, A.G., et al., *J. Mol. Struct.*, 2012, vol. 1014, p. 81.
74. Fukin, G.K., Cherkasov, A.V., Rumyantcev, R.V., et al., *Mendeleev Commun.*, 2019, p. 346.
75. Fukin, G.K., Baranov, E.V., Rumyantcev, R.V., et al., *Struct. Chem.*, 2020, vol. 31, p. 1841.
76. Bader, R.W.F. and Gatti, C., *Chem. Phys. Lett.*, 1998, vol. 287, p. 233.
77. Farrugia, L.J. and Macchi, P., *J. Phys. Chem. A*, 2009, vol. 113, p. 10058.
78. Gatti, C., *Electron Density and Chemical Bonding II*, Stalke, D., Ed., 2012, vol. 147, pp. 193–286.
79. Johnson, E.R., Keinan, S., Mori-Sanchez, P., et al., *J. Am. Chem. Soc.*, 2010, vol. 132, p. 6498.
80. Contreras-Garcia, J., Johnson, E.R., Keinan, S., et al., *J. Chem. Theory Comput.*, 2011, vol. 7, p. 625.
81. Contreras-Garciá, J., Yang, W., and Johnson, E.R., *J. Phys. Chem. A*, 2011, vol. 115, p. 12983.
82. Espinosa, E., Molins, E., and Lecomte, C., *Chem. Phys. Lett.*, 1998, vol. 285, p. 170.

Translated by E. Yablonskaya